Materials Research Express

PAPER • OPEN ACCESS

Photo induced self-diffusion and viscosity in amorphous chalcogenide films

To cite this article: Yu Kaganovskii *et al* 2020 *Mater. Res. Express* **7** 016204

Materials Research Express

PAPER

Photo induced self-diffusion and viscosity in amorphous chalcogenide films

Yu Kaganovskii[1], D L Beke[2], V Freilikher[1], S Kökényesi[3] and A M Korsunsky[4]

[1] Dept. of Physics, Bar-Ilan University, Ramat-Gan 52900, Israel
[2] Dept. of Solid State Physics, University of Debrecen, H-4010 Debrecen, Hungary
[3] Dept. of Electrical Engineering, University of Debrecen, H-4010 Debrecen, Hungary
[4] Dept. of Physics, Kharkov National University of Building and Architecture, Ukraine

E-mail: kagany@biu.ac.il

Keywords: amorphous chalcogenide films, diffusion, mass transfer, viscosity

OPEN ACCESS

RECEIVED
11 October 2019

REVISED
6 January 2020

ACCEPTED FOR PUBLICATION
15 January 2020

PUBLISHED
27 January 2020

Abstract

Acceleration of the mass transport in amorphous chalcogenide films under band gap light illumination is usually attributed to the decrease of the film viscosity. However, our direct measurements of the film viscosity at various temperatures and light intensities, made by flattening of surface relief gratings, have shown that the viscosity did not vary under illumination and the acceleration of the mass transfer was caused by the contribution of photo-induced (PI) self-diffusion. The PI diffusion coefficient is not related to the viscosity coefficient by the Stokes-Einstein relation and PI diffusion should be considered as an additional mechanism of the overall mass transport. In this paper, using well-known models of self-trapped excitons, we present the first atomic interpretation of PI diffusion coefficients, explain their dependence on temperature and light intensity, and compare with our experimental data. For characterization of PI acceleration of the mass transfer we introduce the term 'diffusional viscosity', like it is used for description of diffusion creep in crystalline solids. We estimate the temperature dependence of diffusional viscosity and show that it noticeably depends on the distance over which the material is redistributed. Taking into account the diffusional viscosity allows an adequate general interpretation of many photo-induced phenomena observed in the literature.

1. Introduction

Semiconductor amorphous chalcogenide films (ACF) are subject of substantial scientific and technological interest caused by the possibilities to modify their optical and electric properties by light, electron or ion irradiation (see reviews [1–5]). Some of photo-induced (PI) processes detected in ACF, such as photo-darkening [6, 7], photo-expansion [8], PI fluidity [9–11], PI diffusion [12–14] and mass transport [15–17], are the basis for the fabrication of integrated optical devices, waveguides, surface relief gratings (SRGs), micro-lenses and other elements for micro-optics [18–20].

In this letter, we present the first atomic interpretation of the PI diffusion coefficients, estimate their values as the function of the light intensity, and compare them with the values experimentally determined in our previous studies. We suggest that PI acceleration of the mass transport is caused by the contribution of PI self-diffusion to the total mass transfer process. Thus, the effective PI viscosity measured in the mass transfer experiments, can be called 'diffusional viscosity', - the term commonly used to describe the diffusion deformation of crystalline solids. This interpretation provides a general picture for many photoinduced phenomena observed in the literature.

2. Basic data on PI diffusion coefficients

The first quantitative measurements of PI diffusion coefficients data were obtained using a method based on the theory of capillary flattening of solids [21], which was modified [22] by taking into account the final thickness of

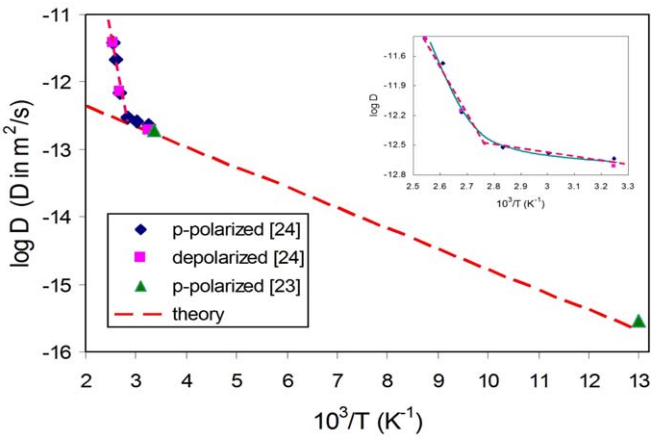

Figure 1. Temperature dependence of PI diffusion coefficients in $As_{20}Se_{80}$ films measured in [23] and [24] for 1.45 W/cm^2 light intensity and estimated by equation (7). Inset: Data obtained in [24] (continuous green line) presented taking into account data of [23] (red dotted lines).

the films. The PI self-diffusion coefficients, D, were measured in $As_{20}Se_{80}$ films *at room temperature* at various light intensities. It was found that D linearly increased with the intensity, I, and the coefficient $\beta = D/I$ was equal 2.5×10^{-18} m^4/J [22]. Later, the PI diffusion coefficients were quantitavely estimated by the kinetics of growth of surface relief gratings (SRGs) at 77 and 300 K [23] for the same film composition, and recently, the PI coefficients were measured [24] in these films in a wide temperature range (308–398 K) and light intensities (0–2.5 W/cm^2). Using the method of capillary flattening of SRGs with two different grating periods, Λ, the authors could separate mechanisms of viscous flow (which was detected near and above glass transition temperature T_g in the dark) and PI self-diffusion (at lower temperatures under band gap laser illumination). All known data on PI diffusion coefficients for $As_{20}Se_{80}$ films are summarized in figure 1 for light intensities at about 1.45 W/cm^2. In [24], the PI diffusion coefficients were presented as non-Arrhenius dependence with the effective diffusion activation energy changing from 0.1 to 0.7 eV as temperature increased (see continuous line in the inset). However, the addition of our low-temperature data [23] led to the temperature dependence of D in the form of two straight lines in the Arrhenius plot, given by equations:

$$D = 1.9 \times 10^{-7} \exp(-0.71 \text{ eV}/kT) \text{ m}^2/\text{s} \quad 353 < T < 398 \text{ K}$$

$$D = 2.2 \times 10^{-16} \exp(-0.06 \text{ eV}/kT) \text{ m}^2/\text{s} \quad 77 < T < 353 \text{ K}$$

3. Atomic interpretation of PI self-diffusion coefficients

Radiation enhanced diffusion and accompanying diffusion-controlled processes have been repeatedly discussed in the context of neutron irradiation of metallic alloys [25]. Two main mechanisms of the diffusion enhancement were identified. On one hand, collisions between energetic neutrons and atoms of the target lead to a forced atomic mixing, which can be well modelled by a *ballistic* diffusion process. On the other hand, nuclear collisions initiate the formation of point defects, whose supersaturation results in an acceleration of *thermal* diffusion. In many situations, ballistic mixing and thermally activated diffusion compete, since they tend to drive the microstructure in different directions: ballistic mixing randomizes atomic configurations, e.g., promotes the disordering of chemically ordered phases or dissolution of parcipitates, while thermally activated diffusion is driven by chemical potential gradient and often results in the formation of ordered phases or precipitates.

Similar processes can occur in ACFs under illumination by the band gap light. Structure of ACFs, such as As_2Se_3 or As_2S_3, represents chains, consisting mainly of P–C bonds (P and C denote pnictide and chalcogen atoms, respectively). With the increase of chalcogene concentration, also C–C bonds appear. Excitation of ACFs by light with appropriate photon energy leads to breakage of P–C and C–C bonds and formation of electron-hole pairs, such as P_2^+–C_1^- and C_1^+–C_1^-, where subscript shows the number of bonds and superscript notes the sign of the charge [26]. These configurations are unstable and transform into more stable valence alternation pairs (VAP), called also as self-trapped excitons (STE), which can be considered as radiation-induced point defects. Formation of these defects can accelerate atomic jumps and thus result in increase of the diffusion coefficients of both chalcogens and pnictides compared to their thermal diffusion without irradiation.

Two ways of such acceleration are possible.

(i) According to Fritzsche [27], the recombination of electron-hole pairs caused by photo-excitation, is mainly nonradiative and is accompanied by dissipation of rather large recombination energy [28]. *After recombination*, bonding configuration can be changed, so that some atoms can move over atomic distances in the local volume where the recombination energy was released. Thus, in this case, the elementary diffusion jump can be associated with the *recombination* event, and both pnictide (*P*) and chalcogene (*C*) atoms may jump, depending on the local configuration. These random jumps are similar to the *ballistic diffusion* in metals under neutron irradiation.

(ii) Another mechanism of light induced acceleration of atomic jumps is caused by the deformation of bonds and appearance of free volumes due to formation of valence alternative pairs. This can enhance *thermal* jumps of both chalcogens and pnictides, whose number per unit volume correlates with the defect concentration, *n*. Since the frequency of jumps and thus the diffusion coefficient are proportional to *n, the thermal diffusion coefficient* increases.

For quantitative estimates, we present the PI diffusion coefficients for pnictide atoms and chalcogens as

$$D_i = \frac{1}{2}\Gamma_i a^2; \quad i = P, C \tag{1}$$

Here, a is the average length of elementary jump, Γ_P and Γ_C are the jump frequencies of the pnictides and chalcogens, respectively, which are determinded either by the probability of recombination near a given atom, $\Gamma_i^{h\nu}$, or by the thermal activation near the existing defect, Γ_i^{th}. We assume for simplicity that under illumination by a linearly polarized light, the diffusion jumps occur preferably along the polarization vector, as it was shown in experiments [9, 15, 16]. This justifies the factor 1/2 in equation (1); in a three-dimensional random walk this factor is 1/6 for isotropic medium.

The ballistic frequencies $\Gamma_i^{h\nu}$ can be estimated as

$$\Gamma_i^{h\nu} \approx \frac{n\bar{\omega}c_i}{\tau}; \tag{2}$$

Here, the product $n\bar{\omega}c_i$ gives a probability to meet an i-atom (P or C) near the defect ($\bar{\omega} = N^{-1}$ is the average atomic volume; N is the total number of atoms per unit volume, $n\bar{\omega}$ is the dimensionless defect concentration, c_i is the atomic fraction of i-atoms, and τ is the defect lifetime; τ^{-1} is the recombination frequency). Similarly to the jump frequency in crystalline solids, which is defined by a product of the vacancy concentration and the vacancy jump frequency, the jump frequencies $\Gamma_i^{h\nu}$ are given by the product of the instantaneous defect concentration $n\bar{\omega}$ and the frequency of the exciton decay τ^{-1}.

The thermally induced frequencies Γ_i^{th} can be written in the usual (Arrhenius-type) form

$$\Gamma_i^{th} \approx n\bar{\omega}c_i\nu_0 \exp(-Q_m^i/kT) \tag{3}$$

where ν_0 denotes the oscillation frequency of atoms, Q_m^i is the migration energy of the i- atom. The thermal induced jumps are possible only due to the existence of free volumes induced by the light. For the determination of n, presented in equations (2) and (3), we note that both jump probabilities are proportional to the defect concentration $n\bar{\omega}$, and n can be estimated from the following equation

$$\frac{dn}{dt} = \chi\frac{\alpha \cdot I}{h\nu} - \frac{n}{\tau} = 0. \tag{4}$$

Here, α is the absorption coefficient of the ACF, I is the light intensity, $h\nu$ is the photon energy, and χ is the efficiency of electron-hole generation. The term $\alpha \cdot I/h\nu$ gives a number of photons absorbed in unit volume per unit time. After some short time, $t \ll \tau$, n is determined by its steady state value

$$n = \chi \ \alpha \cdot I \ \tau/h\nu, \tag{5}$$

and taking into account equations (2) and (3) for the PI diffusion coefficients, we obtain:

$$D_i^{h\nu} \approx \beta_i^{h\nu} I \quad \beta_i^{h\nu} \approx \chi\frac{\alpha \cdot a^2\bar{\omega}c_i}{2 \cdot h\nu} \quad i = P, \ C \tag{6}$$

$$D_i^{th} \approx \beta_i^{th} I \quad \beta_i^{th} \approx \beta_i^{h\nu}\tau\nu_0 \exp(-Q^i/kT). \tag{7}$$

Equation (6) gives the 'ballistic' PI diffusion coefficient, which can be responsible for diffusion mixing under irradiation, whereas equation (7) gives an estimate for 'thermal' PI coefficients.

As it follows from equations (6) and (7), both types of PI diffusion coefficients linearly depend on the light intensity I, as well as on the absorption coefficient α. The 'ballistic' coefficients do not depend on the lifetime τ, because the appropriate jump frequencies are determined by the ratio n/τ [see equation (2)].

4. Comparison with the experiments

The effective PI diffusion coefficients determined from the kinetics of mass transfer experiments can be written as [22]

$$D \approx D_P c + D_C(1 - c) \tag{8}$$

where c is the concentration of P-atoms, D_P and D_C are the diffusion coefficients of the pnictide and chalcogene atoms.

Substituting typical values $a \approx 3 \times 10^{-10}$ m, $\bar{\omega} \approx 5 \times 10^{-29}$ m^3, $h\nu \approx 2$ eV, $\alpha \approx 3\ \mu$m^{-1}, $\chi = 0.1$, $c \approx 0.5$ into equation (6), we obtain $\beta_i^{h\nu} = 1.2 \times 10^{-24}$ m^4/J, which is about 6 orders of magnitude smaller compared to the value (2.5×10^{-18} m^4/J) found in the experiment [22]. For typical intensities used in experiments ($I \approx 1$ W/cm^2) the 'ballistic' coefficient is $D_i^{h\nu} \approx 1.2 \times 10^{-20}$ m^2/s., i.e. it is also much smaller than D obtained in the experiments ($\sim 10^{-13}$ m^2/s), even at 77 K ($\sim 10^{-15}$ m^2/s). Thus, the ballistic diffusion coefficients cannot explain the PI acceleration of the mass transfer obtained in the experiments.

In contrast, thermally activated diffusion coefficients, D_i^{th}, can be much larger than $D_i^{h\nu}$. Substituting $\nu_0 \approx 3 \times 10^{12}$ s^{-1}, the exciton lifetime $\tau \approx 2 \times 10^{-5}$ s, light intensity $I = 1.45$ W/cm^2, and $Q_m \approx 0.06$ eV (for low-temperature branch of D), we obtain a good agreement with the above mentioned experimental values (see dotted line in figure 1). It should be noted that the average exciton lifetime $\tau \approx 2 \times 10^{-5}$ s, taken for these estimates is an order of magnitude longer than it was assumed in [23]. Taking into account larger values of τ, practically did not change the experimentally obtained D values shown in the figure 1. The preexponential factor, D_0, for low-temperature branch in figure 1 is also in agreement with the values measured in the experiments.

At higher temperatures, near and above T_g ($T_g \approx 370$ K for $As_{20}Se_{80}$), coupling of P and C-atoms with electrons and holes, as well as the Coulumb interaction of the diffusing atoms with the charged radiation defects become less probable. On the other side, the atoms located near the radiation defects can overcome regular potential barriers. Thus, the high-temperature branch in the Arrhenius plot can be caused by regular diffusion, which is accelerated (compared to that in the dark) due to high enough concentration of radiation defects. This interpretation can be confirmed by the value of the pre-exponential factor ($D_0 = 1.9 \times 10^{-7}$ m^2/s) in the high-temperature branch of the Arrhenius plot. Usually, the pre-exponential factor is expressed as $D_0 \approx a^2 \nu_0 n \bar{\omega}$, and with $a^2 = 10^{-19}$ m^2, $\nu_0 \approx 3 \times 10^{12}$ s^{-1}, and $n\bar{\omega} \approx 0.1$, we obtain $D_0 = 0.3 \times 10^{-7}$ m^2 s^{-1}. The disagreement with the experiment is due to the fact that the temperature range of the PI diffusion measurements was too narrow.

It is worth to compare our results, shown in figure 1 with those obtained in a very recent paper by Lee and Vlassak [29], in which the authors have found that in metallic CuZr and NiZr amorphous alloys the diffusion below the glass transition temperature followed an Arrhenius type temperature dependence, while the kink on this dependence above T_g illustrated the breakdown of the Stokes-Einstein relation between the viscosity and diffusion. Figure 2 shows the log D versus T_g/T plots for CuZr and NiZr metallic systems, and our data obtained in $As_{20}Se_{80}$. It is seen that the curves have similar features in the sense that they have a break at the temperature $T \approx T_g$ and have an Arhhenious type temperature dependence below T_g. Discussing the results shown in figure 1, we suggested an Arrhenous-type temperature dependence at the high temperatures as well. However, since we have only three points above T_g, it is still unclear whether indeed there is an Arrhenius-type temperature dependence, or the curve for $As_{20}Se_{80}$ has a similar curvature like for metallic systems. This certainly calls for further experiments in this temperature region.

5. PI viscosity

According to our direct measurements of the viscosity coefficients in the dark and under illumination by a band gap light [24], the 'pure' viscosity coefficients practically do not depend on the illumination. Acceleration of the mass transfer under band gap illumination is caused only by the contribution of PI diffusion in the mass transfer process. This contribution leads to a decrease of the effective 'diffusional viscosity', which can be defined as a ratio $\sigma/\dot{\varepsilon}$ where $\dot{\varepsilon}$ is a deformation rate, caused by stress σ [30, 31]. Similarly to other amorphous solids [32, 33], the relation between viscosity and diffusion in solid amorphous chalcogenides noticeably deviates from the Stokes-Einstein equation, due to the difference in molecular mechanisms of viscous flow and diffusion. It is guessed that the dynamics of the viscous flow is heterogeneous coherent motions of chains and rings [32], i.e. it is sliding of structural elements relatively to one another. The sliding is facilitated by the presence of free volumes [34] associated with defects in *inter*molecular bonds, such as, for example, dangling bonds. The diffusion of the atoms, of which the material consists, is caused mainly by *intra*molecular reconstruction (individual atomic hopping events) and thus not immediately related to the viscous flow. The intramolecular reconstruction (atomic diffusion) can also contribute to the shape variation under applied stresses, like it happens in crystalline

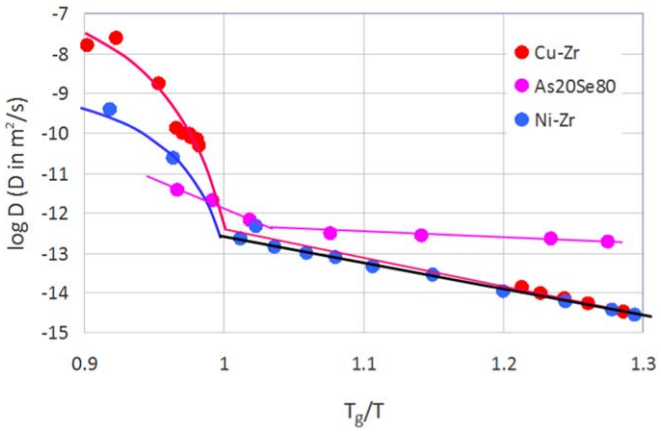

Figure 2. Comparison of our results on PI diffusion coefficients in $As_{20}Se_{80}$ with recent results of Lee and Vlasak [29] on diffusion in solid and overcooled liquid alloys Cu-Zr and Ni-Zr.

solids, in which 'pure' viscosity is negligible. Similarly to crystalline solids, the PI mass transfer in amorphous solid materials can be considered as a diffusional-viscous flow. The increase of the effective PI fluidity during low-temperature mass transfer (so called 'photo-melting' [35]) can also be easily explained in terms of PI diffusion. The same applies to the PI increase of fluidity in nano-indentation experiments [9, 36].

As it was mentioned above, our results on PI diffusion were obtained by measurements of the erasing kinetics for gratings previously recorded on the film surface. According to the theoretical analysis [22], which accounted for both the viscous flow and the bulk diffusion mechanisms, the effective smoothing constant can be expressed as [24]

$$\kappa = C\frac{\pi\gamma}{\Lambda\eta} + B\frac{8\pi^3 D\gamma\bar{\omega}}{\Lambda^3 kT} = C\frac{\pi\gamma}{\Lambda\eta_{eff}}. \tag{9}$$

Here, D is the effective diffusion coefficient, which determines the kinetics of the mass transfer, γ is the surface tension, Λ is the grating period, H is the film thickness, η is the dynamic viscosity, $\bar{\omega}$ is the average atomic volume, k is the Boltzmann constant, $B = 1 - e^{-2\pi H/\Lambda}$ and $C = -e^{4\pi H/\Lambda} \cdot \frac{1 + 4\pi H/\Lambda - e^{4\pi H/\Lambda}}{1 + e^{8\pi H/\Lambda}}$ are numerical coefficients, which depend on the ratio H/Λ, T is the absolute temperature. Equation (9) can be considered as the definition of an 'effective fluidity' proportional to the reciprocal values of the 'effective viscosity', η_{eff}.

If the acceleration of mass transfer is attributed to an increase of PI fluidity, the *effective* viscosity coefficient of the ACFs can be expressed by the formula

$$\frac{1}{\eta_{eff}} = \frac{1}{\eta} + \frac{8\pi^2\bar{\omega}BD}{C\Lambda^2 kT}. \tag{10}$$

Thus, the PI diffusion contribution to the total mass transfer process lowers *the effective viscosity* of the films. As it is seen from equation (10), the effective 'diffusional' viscosity is strongly dependent on the distance (Λ) over which the material is redistributed.

In figure 3(a), we present the dependence of η_{eff} on Λ calculated for different temperatures for the film thickness $H = 2$ μm, with 'pure' viscosity taken from [37] and diffusion coefficients taken from figure 1. The lower the temperature the larger is the increase of η_{eff} with Λ, because diffusion contribution in the mass transport at lower temperatures exceeds for several orders of magnitude the contribution of the viscous flow. In figure 3(b) we show temperature dependence of η_{eff} for $\Lambda = 3$ μm and $\Lambda = 15$ μm. Sharp decrease of η_{eff} near 380 K is caused by sharp increase of PI diffusion coefficient and by a decrease of 'pure' viscosity, η, which at these temperatures becomes comparable with η_{eff}.

6. Conclusion

We propose an atomic interpretation of PI diffusion coefficients in ACFs considering radiation defects as free volumes necessary for diffusion event. We show that the 'ballistic' diffusion coefficients caused by variation in bonding configurations during electron-hole recombination are several orders of magnitude smaller than the 'thermal' PI coefficients of chalcogene and pnictide atoms coupled with electrons and holes. These latter coefficients are in a good agreement with the values obtained in experiments. We explain the effect of the PI

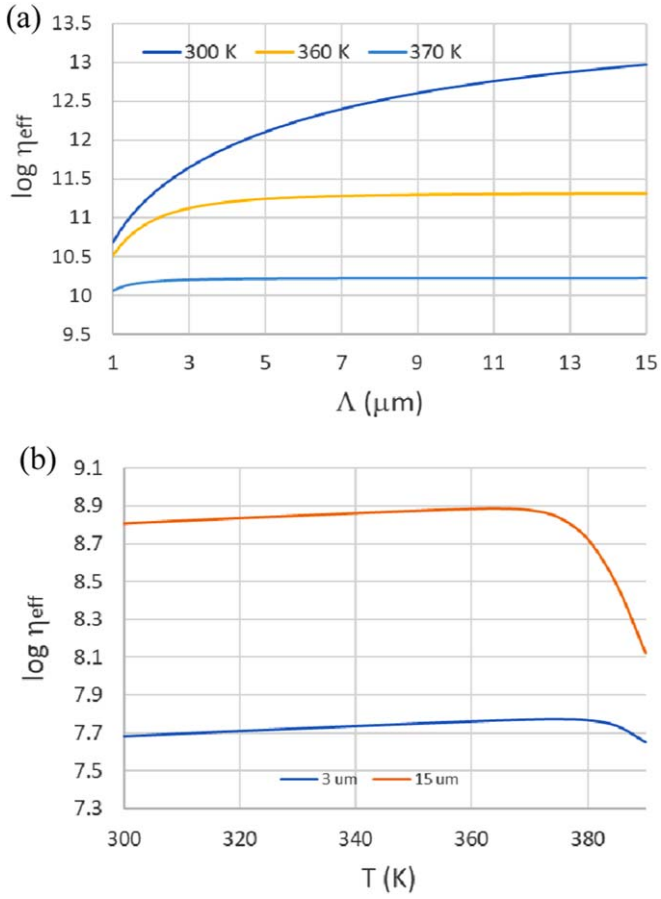

Figure 3. Dependence of the effective viscosity (in Pa × s) on Λ (a) and on the temperature (b) calculated using equation (10).

fluidity considering the contribution of PI self-diffusion to the mass transfer. Our approach, emphasizing the determining role of the diffusion jumps, provides an adequate interpretation of the photo melting. We show that the effective 'diffusional' viscosity is strongly dependent on the distance (Λ), over which the material is redistributed.

Acknowledgments

The work was supported by the GINOP-2.3.2-15-2016-00041 project. The project was co-financed by the European Union and the European Regional Development Fund.

We are thankful to L N Paritskaya for fruitful discussions of our work.

ORCID iDs

Yu Kaganovskii https://orcid.org/0000-0002-8596-8541

References

[1] Elliott S R 1990 *Physics of Amorphous Materials* 2nd Ed (Essex: Longman Scientific &Technical)
[2] Morigaki K 1999 *Physics of Amorphous Semiconductors* (Singapore: World Scientific)
[3] Popescu M A 2000 *Non-Crystalline Chalcogenicides* (Dordrecht: Kluwer) (https://doi.org/10.1007/0-306-47129-9)
[4] Singh J and Shimakawa K 2003 *Advances in Amorphous Semiconductors* (London: Taylor & Francis)
[5] Tanaka K and Shimakawa K 2011 *Amorphous Chalcogenide Semiconductors and Related Materials* (Berlin: Springer) (https://doi.org/10.1007/978-1-4419-9510-0)
[6] Ganjoo A, Shimakawa K, Kamiya H, Davis E A and Singh J 2000 *Phys. Rev.* B **62** R14 601
[7] Mishchenko A, Lindberg G P, Weinstein B A and Reznik A 2014 *Appl. Phys. Lett.* **105** 051912
[8] Hisakuni H and Tanaka K 1994 *Appl. Phys. Lett.* **65** 2925
[9] Trunov M L 2008 *J. Phys. D: Appl. Phys.* **41** 074011
[10] Yannopoulos S N and Trunov M L 2009 *Phys. Stat. Sol.* B **246** 1773

[11] Kastrissios D T and Yannopoulos S N 2002 *J. Non-Cryst. Solids* **299–302** 935
[12] Wagner T, Mackova A, Perina V, Rauhala E, Seppala A, Kasap S O, Frumar M, Mir V and Mil V 2002 *J. Non-Cryst. Solids* **299–302** 1028
[13] Wagner T 2002 *J. Optoelectr. Adv. Mater.* **4** 717
[14] Takats V, Vojnarovich I, Pinzenik V, Mojzes I, Kokenyesi S and Sangunni K S 2007 *Chem. Solids* **68** 943
[15] Saliminia A, Galstian T V and Villeneuve A 2000 *Phys. Rev. Lett.* **85** 4112
[16] Trunov M L, Lytvyn P M and Dyachyns'ka O M 2010 *Appl. Phys. Lett.* **96** 111908
[17] Trunov M L, Lytvyn P M, Nagy P M and Dyachyns'ka O M 2010 *Appl. Phys. Lett* **97** 031905
[18] Viens J-F, Meneghini C, Villeneuve A, Galstian T V, Knystautas E J, Duguay M A, Richardson K A and Cardinal T 1999 *J. Lightwave Technol.* **17** 1184
[19] Ramachandran S and Bishop S G 1999 *Appl. Phys. Lett.* **74** 13
[20] Asobe M, Ohara T, Yokohama I and Kaino T 1996 *Electron. Lett.* **32** 1611
[21] Mullins W W 1959 *J. Appl. Phys.* **30** 77
[22] Kaganovskii Yu, Trunov M L, Beke D L and Kökényesi S 2012 *Mater. Lett.* **66** 159
[23] Takáts V, Trunov M L, Vad K, Hakl J, Beke D L, Kaganovskii Yu and Kökényesi S 2015 *Mater. Lett.* **160** 558
[24] Molnar S, Bohdan R, Takats V, Kaganovskii Yu and Kokenyesi S 2018 *Phys. Status Solidi A* **215** 1800589
[25] Martin G 1984 *Phys. Rev.* B **30** 1424
[26] Elliott S R 1986 *J. Non-Cryst. Solids* **81** 71
[27] Fritzsche H 1998 *Semiconductors* **32** 850
[28] Street R A 1977 *Solid State Commun.* **24** 363
[29] Lee D and Vlassak J 2019 *Scripta Mat.* **165** 73
[30] Nabarro F R N 1948 *Report of a Conference on the Strength of Solids* (London: Physical Society) p 75
[31] Herring C 1950 *J. Appl. Phys.* **21** 5
[32] Faupel F, Frank W, Macht M-P, Mehrer H, Naundorf V, Rätzke K, Schober H R, Sharma S K and Teichler H 2003 *Rev. Modern Phys.* **75** 273
[33] Ediger M D, Harrowell P and Lian Yu J. 2008 *Chem. Phys.* **128** 034709
[34] Cohen M H and Turnbull D 1959 *J. Chem. Phys.* **31** 1164
[35] Poborchii V V, Kolobov A V and Tanaka K 1999 *Appl. Phys. Lett.* **74** 215
[36] Trunov M L and Bilanich V S 2003 *J. Optoelectr. Adv. Mater.* **5** 1085
[37] Molnar S, Bohdan R, Takats V, Kaganovskii Yu and Kokenyesi S 2018 *Mater Lett.* **228** 384